

Fractured pebbles—A new stress indicator

Amir Eidelman, Ze'ev Reches

Department of Geology, Hebrew University, Jerusalem 91904, Israel

ABSTRACT

Well-organized patterns of tensile fractures were found in pebbles of young conglomerates in the Salton trough, California, and in the Dead Sea rift, Israel. The fractures are subparallel to each other in a single pebble and are within numerous pebbles in an outcrop. We show that intrapebble tension could develop due to the amplification of the stresses inside a competent pebble embedded within a compliant matrix; furthermore, tensile stresses may form in the pebbles, even under compressive tectonic stresses. The regional trends of the fractures are consistent in each of the study areas, and they appear to be excellent indicators of the tectonic stresses. The derived angles between σ_{hmax} (the largest horizontal compression) and the dominant local strike-slip fault is about 40° in the En Yahav region of the Dead Sea rift, and about 75° in the Indio Hills area of the Salton trough; these angles are in agreement with other stress data.

INTRODUCTION

Tensile joints are common in many rock types and various tectonic environments. They develop normal to the least compressive stress when the local stresses exceed the tensile strength of the host rock. Systematic joints, however, are rarely observed in poorly cemented conglomerates and sandstones. This infrequent occurrence reflects the tendency of granular rocks to deform by shear and displacement between the rigid grains, and their inability to support high tensile stresses (Mirsa and Sen, 1975; Ching et al., 1989). Therefore, we did not expect to find the well-organized systems of tensile fractures present in the conglomerates of the Salton trough, California, and the Dead Sea rift, Israel. We studied these fractures in the field and analyzed the mechanisms of their formation.

The Salton trough area is characterized by the subparallel San Andreas, Imperial, Brawley, Calipatria, and San Jacinto faults (Crowell, 1987). These faults display right-lateral motion accompanied by intensive subsidence, basin formation, and the accumulation of thousands of metres of unconsolidated sediments (Babcock, 1974). Most clastic sediments in the northern parts of the Salton trough belong to the Mecca Formation (Pliocene), the Palm Spring Formation (Pliocene-Pleistocene), and the Canebrake-Occotillo Conglomerate (Pleistocene), and reach a maximum thickness of 2250 m (Sylvester and Smith, 1987). We measured fractured pebbles in the Mecca Formation in Indio Hills, along the eastern side of the San Andreas fault.

The Arava Valley is part of the Dead Sea transform, south of the Dead Sea. The slip along the transform has been about 105 km and has

been predominantly left lateral since the Miocene (Freund, 1965). Although active left-lateral faults are prominent within the Arava Valley, normal faults form sections of the valley margins. The strike-slip motion occurs along generally north-south en echelon faults and is accompanied by east-west extension of a few kilometres across the transform (Garfunkel, 1981). The extension normal to the transform led to the formation of a conspicuous rift valley filled with medium and coarse clastic sediments of the Hazeva Formation (Neogene) and younger units (Garfunkel, 1981). The thickness of the Hazeva Formation along the margins of the Arava Valley is 50–150 m. Fractured pebbles are common in the conglomerates of the lower member of the Hazeva Formation along the western margins of the rift.

We first describe the fractures, from the single pebble to the regional patterns. The mechanics of pebble fracturing are then addressed by analyzing the stress conditions associated with a rigid inclusion embedded in a compliant matrix. The applicability of the fractured pebbles to tectonic analysis is discussed, and the results are then compared with the tectonic stresses determined by previous structural and geophysical analyses for similar settings.

FIELD OBSERVATIONS

Fractures in a Single Pebble

A typical fractured pebble is a spheroidal to ellipsoidal pebble crossed by two to five subparallel vertical fractures (Fig. 1). The fractured pebbles range in size from 10 to 30 cm; a few boulders are longer than 1 m. The rock types of the fractured pebbles vary: granite, gneiss, schist, and sandstone pebbles are in the Salton trough, and they are primarily limestone and to a lesser degree chert and sandstone in the Dead Sea rift. Some of the fractured pebbles contain preexisting sedimentary or metamorphic foliation, yet the fractures in these pebbles show no apparent modification by the schistosity or the layering.

The observed fractured pebbles contain only one set of systematic fractures. Segmented fractures in an echelon configuration and overlapping zones are abundant. Irregular nonsystematic fractures cut across the intervals between systematic fractures and are roughly normal to them (similar to cross joints of Hodgson, 1961).

The systematic fractures usually have planar surfaces, and some are decorated with curvilinear hackles and ribs that form a plumose structure (Fig. 2). The origins of the plumose structures are located at the margins of the pebbles. This surface geometry resembles that of tensile fractures in well-cemented rocks (Hodgson, 1961; Pollard and Aydin, 1988).

Figure 1. Fractured limestone pebbles embedded in poorly cemented matrix, Arava Valley, Israel. Two to five subparallel joints cut through pebbles.

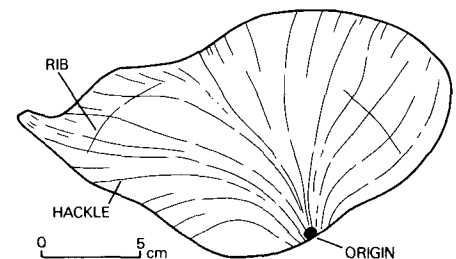


Figure 2. Surface of fracture from limestone pebble, Arava Valley, Israel. Note markings of plumose structure and ribs on surface.

Fracture-parallel displacements are relatively rare; less than 5% of the fractures show such slip. The displacements do not exceed several centimetres, are restricted to individual pebbles, and do not affect neighboring pebbles. Fractures with slip are subparallel to nearby tensile fractures, and the fractures with left-lateral slip are essentially parallel to fractures with right-lateral slip. It appears that the slip occurred in a successive deformation phase along *existing* tensional fractures (similar to the observations of Simpson and Segall, 1986).

Fracture in an Outcrop

In most outcrops, the systematic fractures in separate pebbles are subparallel to each other (Fig. 3). This parallelism appears to be independent of the relative size of the pebbles and the spacing between them (Fig. 3). The fractures are usually restricted to the individual pebbles, and there is no apparent fracture continuity between neighboring pebbles. In well-cemented conglomerates, the fractures are irregular and cut continually through the pebbles and the matrix. Furthermore, the systematic fractures display clear and consistent regional trends in the two study areas.

MECHANISM OF PEBBLE FRACTURING

The observations described above indicate that the fractures are subparallel, vertical surfaces that cut through the pebbles. The fractures are not related to preexisting foliation and they formed in opening mode. The plumose structures and the cleaved geometry of the fracture surface clearly resemble the geometric properties of tensile fractures (Hodgson, 1961; Pollard and Aydin, 1988). Shearing along the fractures is rare and probably belongs to a later stage. We therefore conclude that these fractures formed by tensile failure of the pebbles. Following the common notion, it is assumed that tensile fractures formed normal to the least compressive stress.

The stresses in competent pebbles embedded within a compliant matrix are analyzed here by considering the deformation of a stiff circular elastic inclusion enclosed in an infinite elastic matrix under plane-strain conditions (Fig. 4). This configuration was regarded by Jaeger and Cook (1979, p. 247) as "perhaps the most important single problem in rock

mechanics." The stresses in an inclusion under the above constraints are (Jaeger and Cook, 1979, p. 263, equations 16 and 17):

$$\sigma_{(\max)i} = \sigma_{(\max)r} \frac{[K(X_r + 2) + X_i]K[X_r + 1]}{2[2K + X_i - 1][KX_r + 1]} + \sigma_{(\min)r} \frac{[K(X_r - 2) - X_i + 2]K[X_r + 1]}{2[2K + X_i - 1][KX_r + 1]}, \quad (1)$$

$$\sigma_{(\min)i} = \sigma_{(\max)r} \frac{[K(X_r - 2) - X_i + 2]K[X_r + 1]}{2[2K + X_i - 1][KX_r + 1]} + \sigma_{(\min)r} \frac{[K(X_r + 2) + X_i]K[X_r + 1]}{2[2K + X_i - 1][KX_r + 1]}, \quad (2)$$

and

$$K = \mu_i/\mu_r, \quad X_r = 3-4\nu_r, \quad X_i = 3-4\nu_i, \quad (3)$$

where $\sigma_{(\max)r}$ and $\sigma_{(\min)r}$ are the largest and least compressive remote stress, respectively, $\sigma_{(\max)i}$ and $\sigma_{(\min)i}$ are the largest and least compressive stress, respectively, inside the inclusion, μ_i and μ_r are the shear moduli, and ν_i and ν_r are the Poisson ratios of the inclusion and the matrix, respectively.

The stresses inside a circular or an elliptical stiff inclusion are uniform (Eshelby, 1957). The stresses are generally amplified for $K > 1$, and $\sigma_{(\max)i}$ and $\sigma_{(\min)i}$ becomes asymptotic for $K > 10$. The Poisson ratio of the inclusion ν_i has a small effect, whereas the Poisson ratio of the matrix ν_r has a profound effect on the solutions. Figure 5 displays the intrainclusion stress $\sigma_{(\min)i}$ vs. the remote stress $\sigma_{(\min)r}$ for a very stiff inclusion ($K = 100$, $\nu_i = 0.25$, and ν_r varies). The solutions in regions A and B of Figure 5 show that the intrainclusion stresses are tensile; $\sigma_{(\min)i} < 0$. Region A is of particular interest to pebble fracturing because it shows that the ratio $\sigma_{(\min)i}/\sigma_{(\max)r}$ can attain values as small as -0.5 for $\sigma_{(\min)r}/\sigma_{(\max)r} > 0$. This implies that tensile stresses can develop within a rigid inclusion even under compressive remote stresses. Note also that $\sigma_{(\min)i}$ has smaller values (more tensile) as ν_r approaches 0.5.

We examined the magnitude of the tensile strength of the fractured pebbles by using the fracture toughness approach (Lawn and Wilshaw,

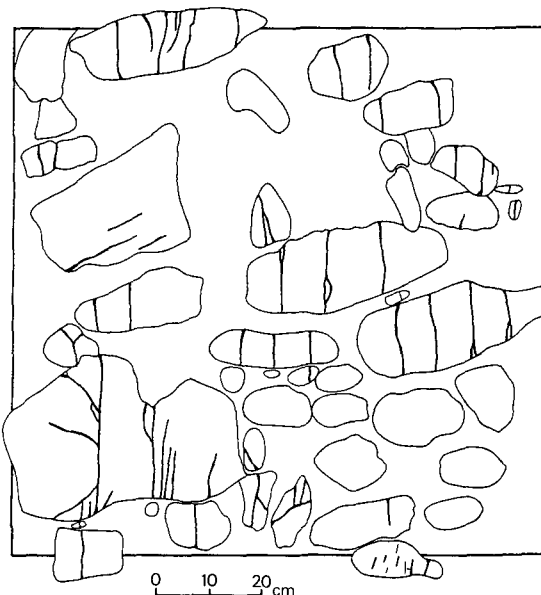


Figure 3. Detailed map of fractured pebbles, Arava, Israel. Note that fractures are restricted to individual pebbles, with no apparent fracture continuity between neighboring pebbles. (Fig. 1 covers central part of this map.)

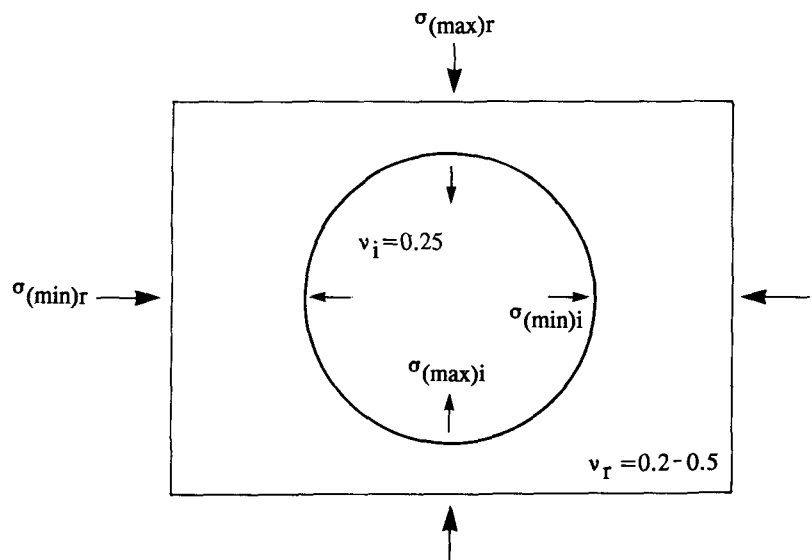


Figure 4. Idealized model for pebble fracturing: rigid elastic circular inclusion in soft matrix under plane strain conditions.

1975). During tensile fracturing (mode I crack), the following relations exist:

$$K_{IC} = (\sigma_3 - P) \gamma (\pi a)^{1/2}, \quad (4)$$

where K_{IC} is the fracture toughness, $(\sigma_3 - P) \gamma$ is the effective stress normal to the crack during yielding, σ_3 is the stress normal to the crack, P is the pore pressure inside the crack, and πa is the length of the initial crack.

Most fractured pebbles are made of limestone, sandstone, granite, and metamorphic rocks; the fracture toughness of these rocks ranges from 0.3 to 1.2 MPa/m^{1/2} (Atkinson and Meredith, 1987). The length of an initial crack is considered to be equal to the grain size (Brace, 1964), which is 2–6 mm in the rocks of our study. For the above-mentioned values of fracture toughness and initial cracks of 2–6 mm long, fracture could develop when $(\sigma_3 - P) \gamma$ is 3–13 MPa. From this strength range we assumed that 5 MPa is a reasonable estimate for the in situ tensile strength (smaller than laboratory strength) of corresponding lithology. This strength of 5 MPa is now compared with the least compressive stress inside the pebble,

$\sigma_{(min)i}$, calculated in the model. Region A in Figure 5 indicates that $\sigma_{(min)i}$ could exceed 5 MPa in a rigid pebble for $0 < \sigma_{(min)r} / \sigma_{(max)r} < 0.1$, if $\sigma_{(max)r} \geq 10$ MPa. The $\sigma_{(max)r}$ component in the model is equivalent to σ_1 , the maximum compressive tectonic stress in the field. Because, in general, σ_1 is equal to or larger than the vertical overburden stress, $\sigma_{(max)r}$ would exceed 10 MPa at depths of about 0.4 km (assuming sediment bulk density of 2500 kg/m³). Therefore, the result of $\sigma_{(max)r} \geq 10$ MPa implies that fracturing occurred under an overburden of a few hundred metres.

DISCUSSION

The striking field observation of this study was the consistency of the fracture orientations (Fig. 3). All examined exposures displayed one set of vertical systematic fractures, and thus they reflect a single tectonic stage. It was shown above that the tensile fractures could form in pebbles at depths of a few hundred metres. Following the notion that tensile fractures form normal to the least compressive stress, we discuss here the applicability of the fractures in pebbles as a tectonic-stress indicator.

The trends of more than 650 fractures were measured at three sta-

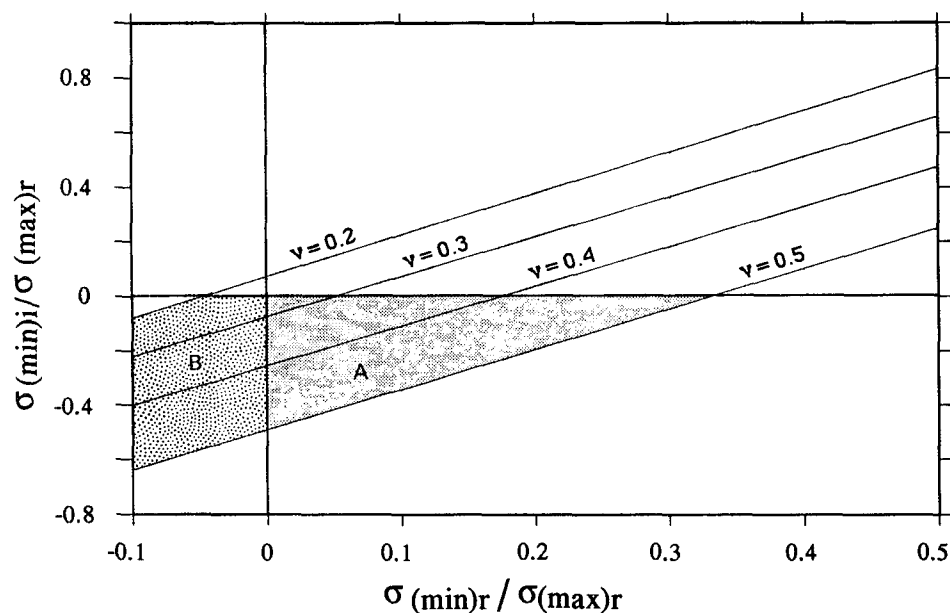


Figure 5. Amplification of tensile stress inside inclusion, $\sigma_{(min)i} / \sigma_{(max)r}$, as function of stress ratio in matrix, $\sigma_{(min)r} / \sigma_{(max)r}$. Calculated after equations in text, for $K = 100$, $\nu_r = 0.2, 0.3, 0.4$, and 0.5 , and $\nu_i = 0.25$.

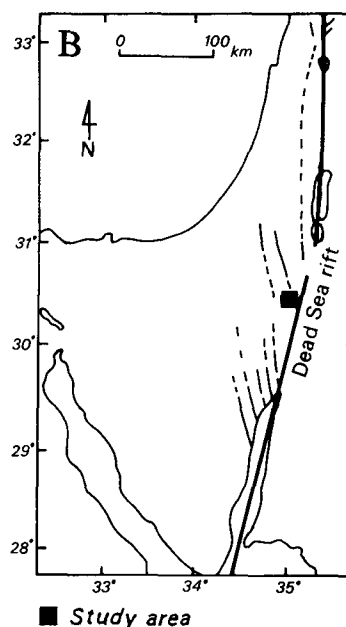
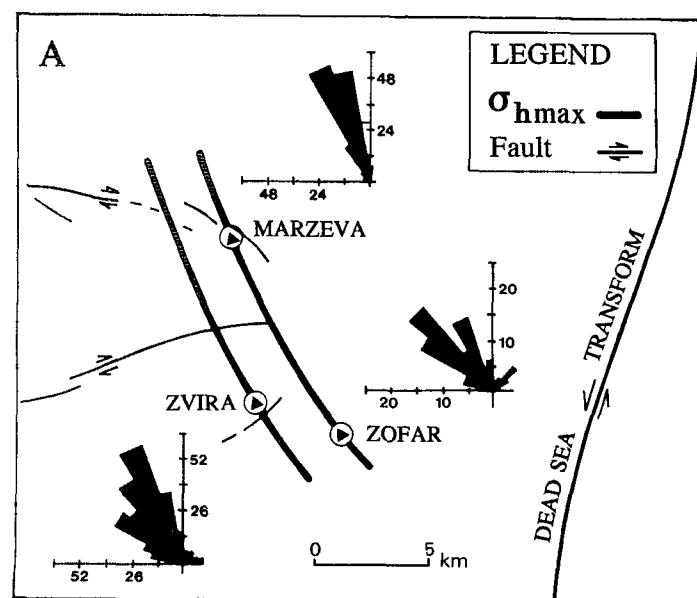


Figure 6. Tectonic stresses and fractures in Arava Valley. A: Strike orientations of fractures (rose diagrams) at three stations (solid triangles). Mean orientations: Marzeva = $334^\circ \pm 12^\circ$ ($n = 191$), Zvira = $332^\circ \pm 19^\circ$ ($n = 361$), Zofar = $328^\circ \pm 18^\circ$ ($n = 101$). Direction of σ_{hmax} (solid, thick lines) drawn according to mean direction of fractures in stations. B: Trajectories of σ_{hmax} (thin lines) along Dead Sea transform as determined from mesostructures (after Eyal and Reches, 1983).

tions in the Arava Valley, Israel. The stations are about 5 km from one another and each station includes at least 15 fractures/m². Almost all fractures are steeper than 80° and the dominant strike of these fractures within each station falls in the range of 333°±17° (Fig. 6A). These results indicate that $\sigma_{(\min)r}$ is horizontal, trending 63°±17°. The regional paleostresses in the Sinai-Israel subplate were determined independently from mesostructures by Eyal and Reches (1983), who showed that the prevailing stress field since the middle Miocene has a σ_{\min} axis (the least horizontal tectonic stress) that trends 70°–80° (Fig. 6B). This trend of the tectonic paleostresses agrees with the range of the trends deduced from the pebble fractures.

The trends of more than 300 fractures were measured in six stations located in the Indio Hills along the southern San Andreas fault (Fig. 7). The stations are within 1 km of the main fault trace and are several hundred metres from each other. The mean strike of the fractures in Indio Hills is 25°±20° (Fig. 7A). Jones (1988) determined the current regional tectonic stress by stress inversion of moderate earthquakes within 10 km of the San Andreas fault. She found that σ_{\max} (the axis of largest horizontal tectonic compression) in the Indio Hills area trends 20° (Fig. 7B), in good agreement with the fracture orientations of 25°±20°.

The consistency of local and regional trends of the fractures in the

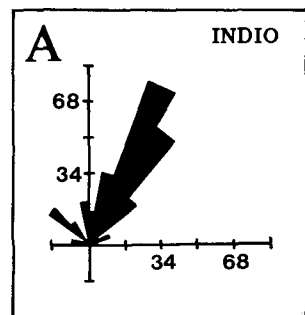
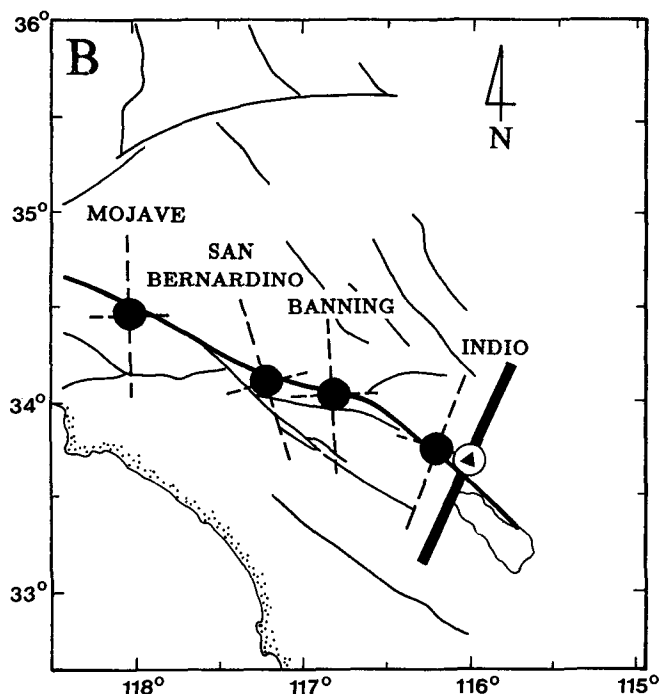


Figure 7. Tectonic stresses and fractures in Salton trough area. **A:** Rose diagram of fracture strikes measured in six stations in Indio Hills along southern San Andreas fault (location marked by solid triangle in B). Mean strike of the fractures is 25°±20° ($n = 340$). **B:** Current regional tectonic stress σ_{\max} (dashed lines) determined by stress inversion of moderate earthquakes within 10 km of San Andreas fault (after Jones, 1988). Solid, heavy line in Indio Hills indicates common orientation of pebble fractures.



pebbles, and their good agreement with tectonic stresses determined independently, indicates that fractured pebbles are reliable indicators of tectonic stresses.

CONCLUSIONS

1. Organized, systematic sets of tensile fractures occur in competent pebbles embedded in poorly cemented conglomerates.
2. The fracturing may be due to the intrapebble amplification of the tectonic stresses, leading to the generation of intrapebble *tensile* stresses. Such stresses may be generated even under a compressive state of stress, provided that $0 < \sigma_3/\sigma_1 < 0.1$.
3. Considering typical tensile strength of rocks, pebbles can fracture at a depth of a few hundred metres or deeper.
4. The consistent regional patterns of fractures in pebbles and their agreement with trends of σ_{\max} determined independently by other investigators show that the fractured pebbles are an excellent indicator of the paleostress orientation.

REFERENCES CITED

- Atkinson, B.K., and Meredith, P.G., 1987, Experimental fracture mechanics data for rocks and minerals, in Atkinson, B.K., ed., *Fracture mechanics of rocks*: London, Academic Press, p. 477–525.
- Babcock, E.A., 1974, Geology of the northeast margins of the Salton trough, Salton Sea, California: *Geological Society of America Bulletin*, v. 85, p. 321–322.
- Brace, W.F., 1964, Brittle fracture of rocks, in William, R.J., ed., *State of stress in the earth's crust*: New York, Elsevier, p. 111–174.
- Ching, S.C., Weeraratne, S.P., and Misra, A., 1989, Slip mechanism-based constitutive model for granular soils: *Journal of Engineering Mechanics*, v. 115, p. 790–807.
- Crowell, C.J., 1987, Late Cenozoic basins of on shore southern California, in Ingersoll, R.V., and Ernst, W.G., eds., *Cenozoic basin development of coastal California*: Englewood Cliffs, New Jersey, Prentice-Hall, p. 207–241.
- Eshelby, J.D., 1957, The determination of the elastic field of an ellipsoidal inclusion, and related problems: *Royal Society of London Proceedings*, v. 241, p. 376–395.
- Eyal, Y., and Reches, Z., 1983, Tectonic analysis of the Dead Sea Rift region since the Late Cretaceous based on mesostructures: *Tectonics*, v. 2, p. 167–185.
- Freund, R., 1965, A model of the structural development of Israel and adjacent areas since Upper Cretaceous time: *Geological Magazine*, v. 102, p. 189–205.
- Garfunkel, Z., 1981, Internal structure of the Dead Sea leaky transform (rift) in relation to plate kinematics: *Tectonophysics*, v. 80, p. 81–108.
- Hodgson, A.R., 1961, Classification of structures on joint surfaces: *American Journal of Science*, v. 259, p. 493–502.
- Jaeger, J.C., and Cook, N.G.W., 1979, *Fundamentals of rock mechanics*: London, Chapman and Hall, 593 p.
- Jones, L., 1988, Focal mechanisms and the state of stress on the San Andreas fault in southern California: *Journal of Geophysical Research*, v. 93, p. 8869–8891.
- Lawn, B.R., and Wilshaw, T.R., 1975, *Fracture of brittle solids*: Cambridge, England, Cambridge University Press, 204 p.
- Mirsa, B., and Sen, B.R., 1975, Stresses and displacement in granular materials due to surface load: *International Journal of Science*, v. 13, p. 743–761.
- Pollard, D.D., and Aydin, A., 1988, Progress in understanding jointing over the past century: *Geological Society of America Bulletin*, v. 100, p. 1181–1204.
- Simpson, C., and Segall, P., 1986, Nucleation of ductile shear zones on dilatant fractures: *Geology*, v. 14, p. 56–59.
- Sylvester, A.G., and Smith, R.R., 1987, Structure section in Painted Canyon, Mecca Hills, southern California, in Hill, M.L., ed., *Cordilleran Section of the Geological Society of America*: Boulder, Colorado, Geological Society of America, Centennial Field Guide 1, p. 103–108.

ACKNOWLEDGMENTS

Supported by the Society of the Protection of Nature in Israel and the Israel–U.S. Bi-National Science Fund, Grant 86-183. We appreciate stimulating discussion with Gidi Baer (Israeli Geological Survey), Amotz Agnon and the late Yuri Liberman (Hebrew University), Mark Zoback (Stanford University), and Yaacov Benvenisty (Tel-Aviv University). We thank Atilla Aydin (Stanford University) and Peter Bird (University of California, Los Angeles) for helpful reviews. We thank especially Vered for her help in the field work and graphic design.

Manuscript received August 26, 1991

Revised manuscript received December 30, 1991

Manuscript accepted January 6, 1992